

The thermodynamical response functions and the origin of the anomalous behavior of liquid water

Francesco Mallamace,^{*acd} Carmelo Corsaro,^a Domenico Mallamace,^b Cirino Vasi^c and H. Eugene Stanley^d

Received 3rd May 2013, Accepted 2nd July 2013

DOI: 10.1039/c3fd00073g

The density maximum of water dominates the thermodynamics of the system under ambient conditions, is strongly P -dependent, and disappears at a crossover pressure $P_{\text{cross}} \sim 1.8$ kbar. We study this variable across a wide area of the T - P phase diagram. We consider old and new data of both the isothermal compressibility $K_T(T, P)$, the pressure constant specific heat $C_p(T)$ and the coefficient of thermal expansion $\alpha_p(T, P)$. We observe that $K_T(T)$ shows a minimum at $T^* \sim 315 \pm 5$ K for all of the studied pressures, whereas, at the same temperature, $C_p(T)$ has the minimal variation as a function of P in the interval 1 bar–4 kbar. We find the behavior of α_p also to be surprising: all the $\alpha_p(T)$ curves measured at different P cross at T^* . The experimental data show a “singular and universal expansivity point” at $T^* \sim 315$ K and $\alpha_p(T^*) \approx 0.44 \cdot 10^{-3} \text{ K}^{-1}$. Unlike other water singularities, we find this temperature to be thermodynamically consistent in the relationship connecting the three response functions. By considering also the P - T behavior of the self-diffusion coefficient D_S and of the NMR proton chemical shift δ we have the information that at T^* the water local order points out, with decreasing T , the crossover from a normal fluid to the anomalous and complex liquid characterized by the many anomalies.

1 Introduction

Water is abundant in the universe and on the surface of the earth where it plays very important roles in most natural phenomena and biological systems. Although water is one of the simplest molecules, it has intriguing behaviors that have not been adequately explained, indeed, water remains a complex material with a large number of anomalies that are counterintuitive.¹

^aDipartimento di Fisica and CNISM, Università di Messina I-98168, Messina, Italy. E-mail: francesco.mallamace@unime.it; Fax: +39 090 395004; Tel: +39 090 6765016

^bDipartimento di Scienze dell'Ambiente, della Sicurezza, del Territorio, degli Alimenti e della Salute, Università di Messina I-98168, Messina, Italy

^cCNR-IPCF, Istituto per i Processi Chimico-Fisici del CNR, Messina, I-98168, Italy

^dCenter for Polymer Studies and Department of Physics, Boston University, Boston, MA 02215, USA

The best known of water's unusual properties are in the liquid state, at ambient pressure, its density ρ and viscosity: below its density maximum (at 4 °C), water expands and becomes more viscous and compressible. Other important anomalous behaviors of the ambient pressure liquid include those associated with such thermal response functions as isothermal compressibility K_T , isobaric heat capacity C_P , and thermal expansion coefficient α_p . At ambient pressure, when these response functions are extrapolated from their values in the metastable supercooled phase of water (located between the homogeneous nucleation temperature $T_H = 231$ K and the melting temperature $T_M = 273$ K), they appear to diverge at a singular temperature ($T_S \approx 228$ K).^{1,2} Another important anomaly of water is represented by its “polyamorphism” in its disordered amorphous state. Water becomes glassy below $T_g \approx 130$ K and in that region can exist in two distinct amorphous forms (*i.e.*, it is “polymorphous”).³ The low-density-amorphous (LDA) and high-density-amorphous (HDA) phases exist below T_g , and by tuning the pressure the system can be transformed back and forth between the two phases.³ In addition, immediately above T_g water becomes a highly viscous fluid and at $T_X \approx 150$ K crystallizes. The region between T_X and T_H is a “No-Man's Land” within which water can be studied only if it is confined in small cavities so narrow that the liquid cannot freeze, or if it is located around macromolecules such as the hydration water around proteins.⁴

Water is thus an exciting research topic, and an enormous number of studies have probed the physical reasons for its unusual properties. A convergence of experimental and theoretical results strongly indicates that the key to understanding water's anomalous behavior is the role played by hydrogen bond (HB) interactions between water molecules. All three principal hypotheses proposed to understand water, *i.e.*, the stability-limit,⁵ the singularity-free,⁶ and the liquid-liquid critical point (LLCP)⁷ scenarios agree in this regard.

This latter approach is based on two assumptions: that water “polyamorphism” exists³ and a clustering process occurs due to the HB in which an open tetrahedrally-coordinated HB network is developed. If we begin with the stable liquid phase and decrease T , the HB lifetime, and the cluster size and stability increase, and this altered local structure continues through the No-Man's Land down to the amorphous phase region (where water is polyamorphic). Hence liquid water has local structure fluctuations, some of which are like those of low density liquid (LDL) and others like those of high density liquid (HDL), with an altered local structure that is a continuation of the LDA and HDA phases.⁷ In HDL, which predominates at high T , the local tetrahedrally coordinated HB structure is not fully developed, but in LDL a more open, “ice-like” HB network appears. Water anomalies can reflect the “competition” between these two local forms of liquid. However, it must be stressed that such a model has been the subject of many discussions and controversies from both the experimental^{8,9} and theoretical point of view.^{10–14}

In addition, the liquid water polymorphic transition is difficult to study as it lies well inside the No-Man's Land, but, as mentioned, the crystallization inside this region can be retarded by confining water within nanoporous structures so narrow that the liquid cannot freeze,^{4,15,16} or by using electrolytic solutions.^{17,18}

The experiments done on water in nanopores^{4,19–21} have shown that, when T is lowered, at a certain point the water HB lifetime increases by approximately six orders of magnitude, suggesting the presence of LDL and HDL inside the supercooled region²² and the location of the so called Widom line (the locus at

which the water response functions are at their maximum values).^{19,21} At ambient pressure, the Widom line is crossed at $T_w(P) \approx 225$ K where: (i) a fragile-to-strong dynamic crossover occurs,^{19,23} (ii) the Stokes–Einstein relation is violated,^{20,24} and (iii) the LDL local structure predominates over the HDL one.^{21,24} These findings on confined water have been confirmed by a number of different experiments^{15,25} and MD studies.^{23,24} Also this latter dynamical transition has alternative explanations. In fact, in a recent MD simulation study, Moore and Molinero,¹² by using the mW water model (the water molecule is modelled as a single particle for which the HB is represented as a short-range anisotropic interaction), highlight that $T \approx 225$ K represents the temperature at which the water crystallization rate is maximum.

As yet there has been no definitive proof on the dominance of a specific hypothesis with respect to the others, and at the same time that the physical reality proposed by confined water exists also in bulk water; thus water's anomalous behavior remains an open scientific question, although recent scattering experiments as a function of the wave vector (Q) and of the energy by exploring the power spectrum $S(Q, \omega)$, on bulk and confined water at ambient pressure, propose on the subject an argument of clarification. On decreasing the temperature, the liquid bulk water undergoes a structural transformation with the onset of an extended hydrogen bond network. Such a structure is at the basis of the marked viscoelastic behavior observed as a well defined frequency (ω) and wave vector dependence of the water sound velocity, and thus of the water response functions. All these observed properties appear consistent with the water polymorphism. Under these viscoelasticity conditions (or sound velocity dispersions) the water thermal response functions and their corresponding fluctuations remain finite at ambient pressure.²

Despite these numerous experiments and MD simulations focused on investigating water anomalies and polymorphism, there are still many open questions regarding the chemical physics of the stable liquid in the T – P phase diagram.¹ For example: why does bulk water have complex behaviors, and is there or not a region in which water behaves as a normal liquid? The focus of this work is on answering this question by considering experimental data only inside the stable liquid phase far from the metastable supercooled phase.

Here we attempt to clarify such a situation by taking into account the bulk water data of thermodynamical response functions (ρ and K_T , expansivity α_P , pressure constant specific heat C_P), of transport parameters (viscosity η , self-diffusion coefficient D_S) and of the proton NMR chemical shift as a function of both temperature and pressure. In this way we test, across a wide area of the T – P phase diagram, the connection between water anomalies and the local molecular order dominated by HB networking. For the thermodynamical functions we make use of literature data, whereas the NMR data come out from a new experiment.

The starting point of our analysis is the behavior of the density as a function of pressure and temperature. The situation is illustrated in Fig. 1, where it is very interesting to note that one of the most important water anomalies, *i.e.*, the density maximum that dominates system thermodynamics under ambient conditions, is strongly P -dependent. If we increase P , the density maximum moves to a lower T (*e.g.*, at $P = 1$ kbar it is $T \sim 245$ K). Fig. 1 shows the overall changes of the density $\rho(T, P)$ and clearly indicates this behavior; the reported data^{26–33} refer essentially to bulk and emulsified water (with water droplets of size 1–10 μm).³³ Note that: i) in addition to being P -dependent, the density maximum disappears

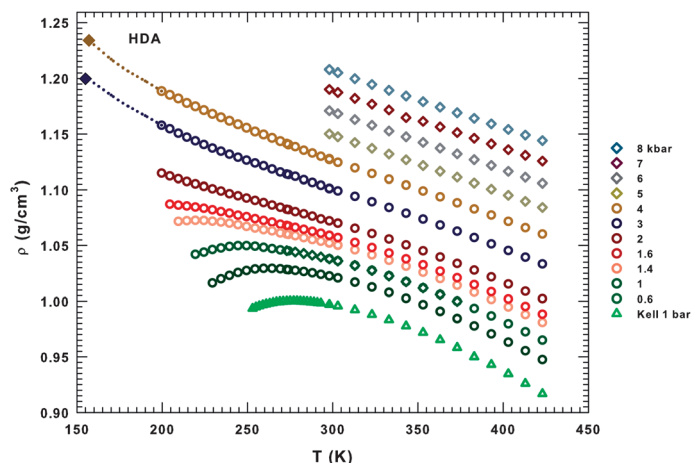


Fig. 1 The bulk water density ρ as a function of T and P , in the intervals $150 < T < 450$ K and $1 \text{ bar} < P < 8$ kbar, respectively.^{26–34} Two main behaviors can be observed: i) the density maximum temperature is P -dependent and disappears for $P > 2$ kbar; ii) the P increase is accompanied by a complete change in the $\rho(T)$ curvature (from negative to positive) at such pressure. Two density values measured in HDA respectively at 3 kbar and 4 kbar are also reported.

for $1.6 < P < 2$ kbar ($P \approx 1.8$ kbar); ii) just at this pressure there is a complete change in the $\rho(T)$ curvature from negative to positive. Fig. 1 also shows the two HDA density values at ~ 155 K measured at 3 kbar and 4 kbar showing a continuity between these values and the bulk water data (dotted lines). Although these HDA densities measured at very high pressures are of the order of 1.2 g cm^{-3} (or even higher), the value of the LDA density measured at 1 bar and 130 K is $\sim 0.94 \text{ g cm}^{-3}$, a value consistent with the confined water ρ values (MCM nano-tubes) inside the No Man's Land, where a density minimum is also seen at $T \sim 200$ K.³⁴

From this complex $\rho(T, P)$ behavior we note that, because the water density maximum is strongly P , T dependent and disappears at a certain crossover pressure ($P_{\text{cross}} \sim 1.8$ kbar), our understanding of the thermodynamic relevance of the density maximum must be adjusted. Perhaps this crossover pressure and some quantity related to $(\partial\rho/\partial T)_P$ has a physical significance we do not yet understand.

2 Results and discussion

2.1 The isothermal compressibility

On the basis of the complex behavior of the liquid water density (mainly in bulk water) illustrated in Fig. 1, here we consider the isothermal compressibility K_T ($K_T = (\partial \ln \rho / \partial \ln P)_T = -V^{-1}(\partial V / \partial P)_T$) in the same P and T intervals previously reported for $\rho(T, P)$. Fig. 2 shows the literature data of $K_T(T, P)$,^{26,28,29,33,35–37} which, as is well-known, is related to volume fluctuations δV as $K_T = \langle \delta V^2 \rangle_{P,T} / k_B T V$. Inspecting the data we see (i) two distinct K_T behaviors in the high and low T regimes, (ii) for the pressures in the $1 \text{ bar} < P < 4$ kbar range the corresponding $K_T(T)$ curves show a minimum (red dots) that is located at $T^* \sim 315 \pm 5$ K, and (iii) as

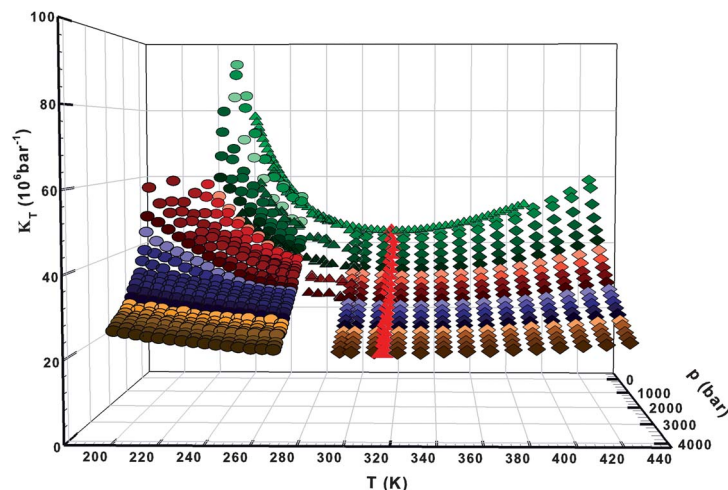


Fig. 2 The bulk water isothermal compressibility $K_T(T, P)$. The colors of the symbols are the same as used in Fig. 1.^{26,28,29,33,35–37} A simple data inspection shows: i) two distinct behaviors of the K_T dependence, at the different pressures, in the high and low temperature regimes; ii) at all the reported pressures, the $K_T(T)$ curves present a minimum value located at the same temperature $T^* \sim 315 \text{ K} \pm 5 \text{ K}$; iii) also for K_T , like for ρ , it seems that P_{cross} is at the borderline of two regions with different volume fluctuations: one where $\langle \delta V^2 \rangle$ is comparable with that of the liquid in its stable phases and the other ($P < P_{\text{cross}}$, and $T < T^*$) with comparatively larger fluctuations.

observed for ρ , for K_T , P_{cross} is the borderline between two regions: one with fluctuations $\langle \delta V^2 \rangle$ comparable to those of liquid in its stable phases and the other with comparatively larger fluctuations in volume ($P < P_{\text{cross}}$, and $T < T^*$). Regarding the (i) and the (iii) items, Fig. 2 clearly shows that the P effect on K_T in the low P - T regime (including the supercooled phase) is more and more pronounced than that in the high- T region ($T > T^*$). This is due to the HB network structure (characteristic of the supercooled region and the primary factor behind water's anomalies), which is less dense and more compressible than at high T . This supports the assumption that the LDL water phase is more pronounced in the low T regime, and the HDL in the high T regime.

2.2 The specific heat

Fig. 2 shows data indicating that the onset of the LDL (*i.e.*, the HB network) occurs near T^* . The T -dependence of the specific heat, measured in the same pressure interval ($1 \text{ bar} < P < 4 \text{ kbar}$ ³⁸) of the K_T and reported in Fig. 3, confirms that T^* can have a special thermodynamical role. Fig. 3 also shows, as little blue dots, C_p data measured in the supercooled regime at $P = 1 \text{ bar}$.³⁹ As it can be observed just around this latter temperature, C_p has minimal variation as a function of the pressure (ΔC_p) if compared with the corresponding values for $T \leq T^*$. In particular, as well evidenced in the figure, the relative pressure variation ΔC_p is larger in the low temperature regime (including the supercooled phase) than that observed in the region $T > T^*$. On considering, hence, that $C_p = (\partial Q / \partial T)_P = T(\partial S / \partial T)_P = \langle \delta S^2 \rangle / k_B$ (where $\langle \delta S^2 \rangle$ are the entropy fluctuations), T^* represents the borderline between two regions: one in which the entropic fluctuations, at the different pressures, increase

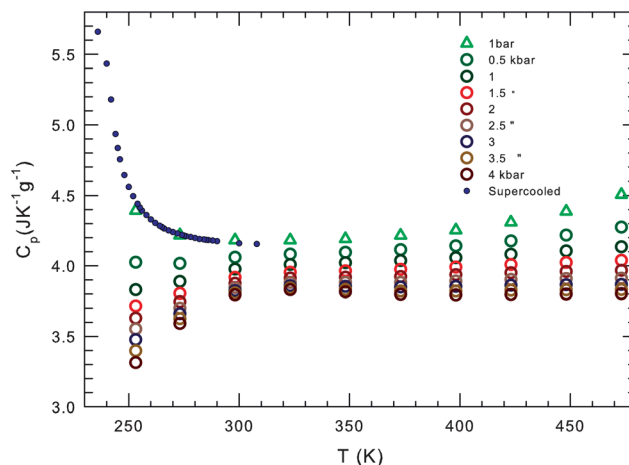


Fig. 3 The pressure constant specific heat $C_p(T)$ in the same T, P intervals of the previous figure. The figure also shows, as little blue dots, the C_p data measured in the supercooled regime at $P = 1$ bar.³⁹ As it can be observed just around T^* , C_p has minimal variation as a function of the pressure.

by increasing T and another one with opposite behaviors in the low temperature and supercooled regimes. In particular for $T > T^*$ and for $P > P_{\text{cross}}$, it can be observed that the C_p behavior is nearly constant; only for $P < P_{\text{cross}}$ does the specific heat data show a slow increase by increasing T . Whereas, in the opposite case, $T < T^*$, C_p , and thus $\langle \delta S^2 \rangle$, presents a considerable temperature variation with decreasing T at all the reported pressures characterized by different behaviors below and above $P \sim 0.5$ kbar: whereas in the first case C_p increases by decreasing T , in the second case it decreases.

2.3 The coefficient of thermal expansion

All these three figures (Fig. 1, Fig. 2 and Fig. 3) evidence the role of the thermodynamical response function derivative as a function of T . The latter two (Fig. 2 and Fig. 3) seem to indicate that in the phase region $T > T^*$ and $P > P_{\text{cross}}$, liquid water behaves like a normal simple fluid. Hence we consider the coefficient of thermal expansion $\alpha_P = -(\partial \ln \rho / \partial T)_P = -V^{-1}(\partial S / \partial P)_T$, representing the entropy and volume cross-correlations $\langle \delta S \delta V \rangle$ to be $\alpha_P = \langle \delta S \delta V \rangle / k_B T V$. Regarding this function, note that, in simple liquids, δS and δV fluctuations become smaller as T decreases and are positively correlated, whereas in water they become more pronounced and, for $T < 277$ K at ambient P , they are anticorrelated.¹ The local order in water is the microscopic cause of these behaviors. As for compressibility and constant pressure specific heat, the P - T behavior of α_P is surprising and, as shown by Fig. 4, T^* is the border between two different behaviors. In the large P -range explored, all the $\alpha_P(T)$ curves measured at different pressures (in the interval from 1 bar to 8 kbar) cross, within the error bars, at the same temperature T^* . Specifically, the experimental data show a “singular and universal expansivity point” at $T^* \sim 315$ K and $\alpha_P(T^*) \approx 0.44 \times 10^{-3} \text{ K}^{-1}$. From these data we have the confirmation that, for $T > T^*$, the thermodynamic behavior of water is exactly the same as that of a normal fluid for all the available P - T values. A situation

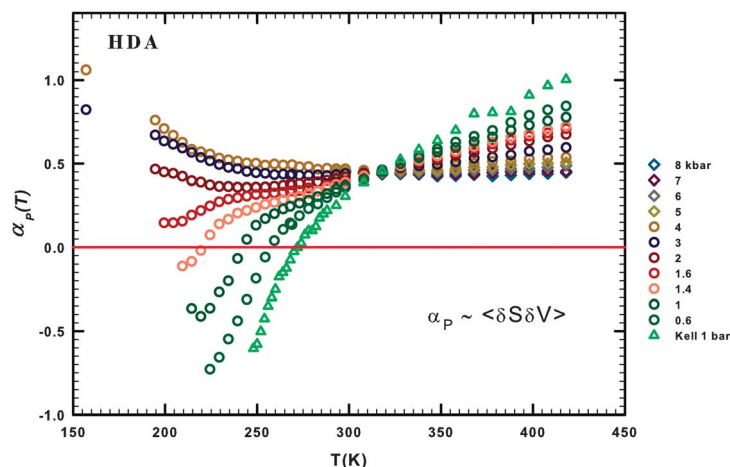


Fig. 4 The bulk water coefficient of thermal expansion $\alpha_p(T)$ in the same T, P intervals of the previous figures. It is clearly observable that all the $\alpha_p(T)$ curves, evaluated at a certain pressure, cross at the same point: $T^* \sim 315$ K with $\alpha_p(T^*) \approx 0.44(10^{-3}K^{-1})$.

that changes in the remaining regions of the phase diagram where, as a function of P , different behaviors are observed. For $P > P_{\text{cross}}$ the δS and δV fluctuations are positively correlated but for $T < T^*$ they increase as T decreases. For $P = 3$ kbar and $P = 4$ kbar there is an apparent continuity between bulk water and its HDA phase. For $P < P_{\text{cross}}$ the $\alpha_p(T)$ evolution is more complex, *i.e.*, $\alpha_p(T)$ decreases as T decreases and, when $P < 1.6$ kbar, anticorrelation processes appear. According to the data, $\alpha_p(T)$ decreases up to a certain flex point and, after a further decrease in T , goes to a minimum whose value decreases as the pressure increases. The exact values and T -positions of these minima (for $P < P_{\text{cross}}$) are not clearly defined in the bulk water data for $\alpha_p(T)$, but their overall behavior seems fully consistent with a data evolution similar to that observed in confined water. In the case of confined water such a minimum temperature is coincident with that of the fragile-to-strong dynamical crossover and of the Widom line, which at ambient pressure is $T_W(P) \approx 225$ K, the same temperature in which C_p has a maximum.²

The reported data and in particular the expansion coefficient behavior for $T > T^*$ is enough to clarify the water properties from a thermodynamical point of view by considering that these data represent the entropy and volume cross-correlation. As mentioned above, two different behaviors are present in $\langle \delta S \delta V \rangle / k_B T V$ for pressures above and below P_{cross} . Note that anticorrelations are possible only for $P < P_{\text{cross}}$, and that the maximum anticorrelation strength occurs at ambient pressure, decreases with increasing P , and vanishes at P_{cross} . This is clearly linked to the HB networking process that characterizes the local order of water: as T decreases inside the supercooled regime, it affects the growth (with increasing stability) of the molecular water structure and gives rise to a sudden entropy decrease. In contrast, pressure effects cause a progressive decrease in HB clustering. It must also be noticed that, for $T < T^*$, the T -behaviors of $\alpha_p(T)$ and $C_p(T)$, both related with δS , are characterized by analogous curvatures; the only difference is in the opposite sign. The density maximum characterizing water disappears near P_{cross} after which the system behaves as a normal liquid. This is a

strong indication that the HB network, *i.e.*, the dynamic water clusters organized in a tetrahedral structure, has a low-density local order. If the presence of this HB network, as far as the behavior proposed by the $\alpha_P(T)$ data (Fig. 3), is or is not consistent with the LLCP approach does not matter with our study; instead, summarizing all the proposed results, here we stress that the water singular temperature T^* has a precise thermodynamical consistence lying in the relationship connecting two of the studied response functions:

$$\left(\frac{\partial\alpha_P}{\partial P}\right)_T = - \left(\frac{\partial K_T}{\partial T}\right)_P \quad (1)$$

Note that T^* represents the liquid bulk water isothermal compressibility minimum temperature and also the crossing point of all the thermal expansion functions in the large phase diagram area, *i.e.*, $200 \text{ K} < T < 430 \text{ K}$ and $1 \text{ bar} < P < 8 \text{ kbar}$.

2.4 The self-diffusion coefficient and the configurational entropy

To have a further confirmation on the proposed entropy role, now we consider the self-diffusion coefficient $D_S(T, P)$ data. This is a dynamic quantity from which we can determine additional information about T^* . Fig. 5(a) shows D_S measured in bulk water as a function of the pressure ($1 \text{ bar} < P < 10 \text{ kbar}$) at several temperatures also in the supercooled regime $252 \text{ K} - 400 \text{ K}$. The $D_S(T, P)$ data in the interval $252 \text{ K} < T < 290 \text{ K}$ are measured using Nuclear Magnetic Resonance (NMR).⁴⁰ The data for $T > 300 \text{ K}$ assume the validity of the Stokes–Einstein relation and are derived from viscosity data available in the literature.⁴¹ Note that, in the

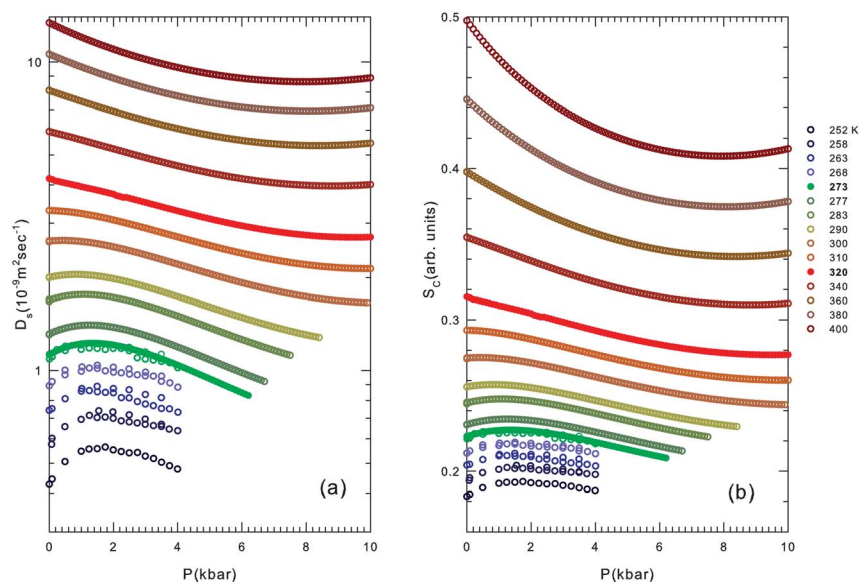


Fig. 5 a) The bulk water self-diffusion coefficient D_S as a function of the pressure in the range $1 \text{ bar} < P < 10 \text{ kbar}$ at different T from the supercooled region 252 K to 400 K . b) The corresponding configurational entropy S_C evaluated according to the Adam–Gibbs approach.⁴⁸ Note that, in both cases, $T^* \sim 315 \text{ K}$ and P_{cross} mark the crossover between two different physical realities.

dynamics of the system, $T^* \sim 315$ K marks the crossover between two different physical realities: below T^* the self-diffusion coefficient has a maximum that for $T = 252$ K is located at ≈ 1600 bar and that, as T increases, evolves at the lowest P and disappears near T^* . When $T > T^*$, the $D_S(P)$ behavior is more regular. In a previous study we have considered these data at constant P in an Arrhenius plot ($\ln D_S$ vs. $1/T$).⁴² We have observed that for all the studied pressure range T^* marks two different regions: for $T > T^*$ the thermal behavior of the self-diffusion coefficient is simply Arrhenius ($D_S = A \exp(E/k_B T)$), but in the temperature range from T^* to the supercooled region (the lowest T is 252 K) the behavior is super-Arrhenius. The Arrhenius activation energy ($T > T^*$) obtained from the data fitting is $E = 15.2 \pm 0.5$ kJ mol⁻¹, *i.e.*, the HB energy value, that fully supports the primary role of HBs in the properties of water. Hence T^* marks a transition from a high- T region characterized by water dynamics with only one energy scale (the Arrhenius energy) to another typical of supercooled glass-forming liquid systems in which the T decreasing causes increasing intermolecular interactions (correlations in the time and length scale, *i.e.*, dynamic clustering). In the water case this is the onset of the HB tetrahedral network.

As in complex liquids, the interaction process originates in the disordered and finite correlation regions (finite polydisperse dynamic clustering) reflected in the transport parameters (relaxation times, viscosity, and self-diffusion) by means of a super-Arrhenius behavior or a multi-relaxation in the time evolution of the density–density correlation functions. Liquid state theory suggests the presence of an onset temperature marking a crossover from normal liquid behavior to supercooled liquid behavior.^{43–47} Above that the transport is Arrhenius and below that correlations cause activation barriers to grow with an increasing scale resulting in super-Arrhenius behavior: *i.e.* a change in the explored configuration space.^{43,46–48} An analogous behavior can be observed as a supercooled liquid approaches the dynamical arrest, starting from a situation like that of a complex material in which its properties are dominated by local potential minima in its energy landscape.^{46,49} A liquid in normal conditions experiences local dynamics in the interaction basins surrounding the minima, and rearranges *via* intra-basin motions and relatively infrequent inter-basin jumps. As the temperature decreases approaching the glass transition, like for the clustering process dominating the complex material dynamics, such jump dynamics become dominant with respect to the intra-basin dynamics and in addition, the molecular interactions impose a levelling in the energy barriers. At this time the dynamics is inverted from super-Arrhenius to pure-Arrhenius, giving rise to a dynamical crossover characterizing the glass-forming liquids.⁵⁰

However, also in the actual case of the transport parameter illustrated in Fig. 5a, the observed behavior can be coherently compared with the case of the thermodynamical functions in terms of the entropic behavior by means of a simple relation originally developed to study glass-forming supercooled liquids: the well known Adam–Gibbs equation.⁴⁸ The equation is developed by considering the reduction in the configurational space as the liquid cools by predicting that the configurational entropy, S_C (a sort of measure of the local order sampled by the liquid molecules) is related to the self-diffusion constant D_S , as:

$$\frac{1}{D_S} = \frac{1}{D_{S0}} \exp(C/TS_C) \quad (2)$$

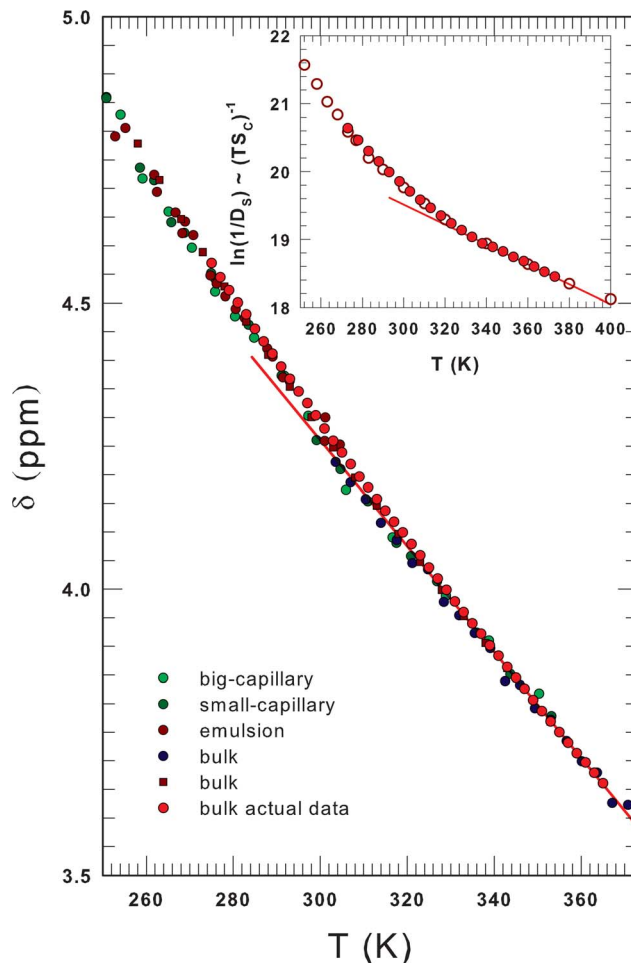


Fig. 6 The bulk water chemical shift $\delta(T)$ measured at ambient pressure in the range 250–370 K in bulk water and in three different samples: big (80–120 μm) and small (10–20 μm) capillaries, and water confined in an emulsion.⁵⁹ The inset shows the results of the Adam–Gibbs linearity relation between $\ln(1/D_s)$ and $(TS_C)^{-1}$.⁴⁸ As described in the text both $\delta(T)$ and S_C represent the atomic local order.

where $1/D_{S0}$ is a prefactor and C a constant. If we assume that the Adam–Gibbs equation is valid, in the water case also at high temperature we can treat the self-diffusion data of Fig. 5a in terms of the suggestions coming out from the overall behavior characterizing K_T , C_p and α_p for which the HB molecular order governs the water physics. Such an idea is also supported by a MD calculation, in terms of the SPC/E potential, of the configurational entropy at points spanning a large region of the T - ρ plane ($210 < T < 300$ K and $0.9 < \rho < 1.4$ g cm⁻³), for which the water diffusive dynamics is essentially governed by the S_C .⁵¹ Hence, by using the latter equation we estimate the S_C behavior by using the D_s data of Fig. 5a. The results are plotted in Fig. 5b where an expected behavior can be observed: S_C mimics the P - T changes of D_s . The surprising situation comes out from the comparison with the MD simulation results: the measured $S_C(P, T)$ confirms all

the findings of the MD evaluation of $S_C(\rho, T)$. First of all these results ensure the validity also for the high- T regime of the linear regression between $\ln D_S$ and $(T_{S_C})^{-1}$ theoretically proposed and experimentally verified in the supercooled regime in a smaller D_S range.⁵² In addition, the $S_C(P, T)$ behavior illustrated in Fig. 5b gives us simple and direct information on the way in which the local order (and hence the HB) changes also showing that T^* represents, even for the configurational entropy, a crossover from two very different regimes. For $T < T^*$ we also see that, in this case, the crossover pressure (P_{cross}) marks two regions of different behavior: by decreasing the pressure from the highest values, the configurational entropy progressively increases with a maximum just around P_{cross} and below which it decreases. Whereas for $T > T^*$, S_C essentially increases by decreasing P . This is a further good representation of the previous results giving a direct illustration on the role of the order (or the disorder) played in all regions of the liquid water phase diagram. In other words the $S_C(P, T)$ behavior illustrated here confirms that ordered HB structures are possible in the water liquid phase only below T^* .

In this section by using the NMR technique (pulsed field gradient spin echo (PGSE) method) by means of a 700 MHz spectrometer we have detailed the self-diffusion coefficient D_S data at ambient pressure in the range $273 < T < 373$ K with steps of 5 K. This is for a direct comparison with the S_C behavior coming out from the measurement, by means of the same technique, of the proton local order discussed in the next section.

2.5 The proton local order

The previous discussion has been based on the consideration that from the self-diffusion data we can obtain information on the local order of a liquid system. There is however another experimental approach that probes more directly the local order observed by a single atom of a given material: the Nuclear Magnetic Resonance (NMR) and more precisely the proton chemical shift δ . It is demonstrated that, if an isolated water molecule in a dilute gas is taken to be the reference for δ , the chemical shift represents the effect of the interaction of water with the surroundings providing, in particular, a rigorous picture of the intermolecular geometry.⁵³ More precisely, it is widely accepted that δ represents the average number of hydrogen bonds (HB) in which a water molecule is involved at a certain temperature.

It is well known that the chemical shift δ is an assumed linear response of the electronic structure of a system under investigation to an external magnetic field B_0 , as $B(j) = (1 - \delta_j)B_0$, where j is an index identifying the chemical environment.^{54,55} It is measured in an NMR experiment by the free induction decay (FID), and specifically it is related to the magnetic shielding tensor σ , which in turn relates to the local field experienced by the magnetic moment of the observed nucleus. The magnetic shielding tensor σ , strongly dependent on the local electronic environment, is a useful probe of the local geometry; and in particular for the hydrogen bond structure for water and aqueous systems and solutions.⁵⁶ On this basis, δ is experimentally obtained by means of a precise procedure.^{53,57} In order to verify the way in which the water local order evolves around T^* , we have performed an NMR experiment in bulk water in the interval $275 < T < 365$ K, at $P = 1$ bar. This is the first experiment of a series of studies on $\delta(P, T)$ in the entire

phase diagram in which the thermodynamical response functions considered here have been studied.

Fig. 6 shows our $\delta(T)$ data (red dots) measured for the present study, after the proper corrections for the density and magnetic susceptibility $\chi(T) = \chi_0 \rho(T)$. Fig. 6 together with our data, also shows all the experimentally available $\delta(T)$ data in the temperature range of stable bulk liquid water,⁵⁸ as well as the δ values from $T = 370$ K down to 250 K, of three different samples: big (80–120 μm) and small (10–20 μm) capillaries, and water confined in an emulsion.⁵⁹ It can be seen in the figure that there is good agreement, within experimental error, between our data and the previous $\delta(T)$ measurements. From the data behavior as a function of the temperature, a linear behavior can be observed only in the range 320–370 K (the red line is generated by a data fitting in the range 325–370 K), for the lowest temperatures a significant deviation from the linear behavior can be observed that means an increase in the water local order. In the inset of the Fig. 6 we have shown a plot of the $\ln(1/D_s) \sim (TS_C)^{-1}$ versus T , evaluated in the range 250–400 K. As seen, the corresponding data from 320 K to 400 K are easily linearly fitted obtaining the red line shown. The correspondence between these results represents, in our opinion, a significant proof from the local atomic point of view, that T^* really represents for water the crossover, by decreasing T , from a normal fluid to the complex liquid characterized by the many anomalies.

3 Conclusions

The reported picture, derived from the thermodynamical functions, transport and local order data, represents the aspect of the chemical–physical reality that characterizes the thermodynamical and structural properties of bulk water by means of the singular temperature and the crossover pressure, respectively T^* and P_{cross} . However the importance of T^* in water can be fully evaluated only by considering in a unitary way all the studied quantities. In particular, on looking to the atomic local order we can clarify that, from the structural point of view, T^* may be the onset temperature of the HB clustering, the point at which liquid water becomes a complex material. In addition, the experimental data, the large P – T phase diagram, and the thermodynamic consistency shown in eqn (1), all indicate that T^* plays a primary role in the physics of water and is the source of its anomalies.

Acknowledgements

The research in Messina is supported by the University of Messina. CC thanks the Fondazione Frisone for its support. The research at Boston University is supported by the NSF Chemistry Division (grants CHE 1213217, CHE 0911389 and CHE 0908218).

References

- 1 *Water Polymorphism: Advances in Chemical Physics*, ed. H. E. Stanley, Wiley, NY, 2012.
- 2 F. Mallamace, C. Corsaro and H. E. Stanley, *Proc. Natl. Acad. Sci. U. S. A.*, 2013, **110**, 4899–4904.
- 3 O. Mishima, L. D. Calvert and E. Whalley, *Nature*, 1985, **314**, 76–78.
- 4 F. Mallamace, P. Baglioni, C. Corsaro, J. Spooren, H. E. Stanley and S. H. Chen, *La Rivista del Nuovo Cimento*, 2011, **34**, 253–388.
- 5 R. J. Speedy and C. A. Angell, *J. Chem. Phys.*, 1976, **65**, 851–858.

- 6 S. Sastry, P. G. Debenedetti, F. Sciortino and H. E. Stanley, *Phys. Rev. E: Stat. Phys., Plasmas, Fluids, Relat. Interdiscip. Top.*, 1996, **53**, 6144–6154; H. E. Stanley, *J. Phys. A*, 1979, **12**, L329–L337.
- 7 P. H. Poole, F. Sciortino, U. Essmann and H. E. Stanley, *Nature*, 1992, **360**, 324–328.
- 8 C. Huang, *et al.*, *Proc. Natl. Acad. Sci. U. S. A.*, 2009, **106**, 15214–15218.
- 9 G. N. I. Clark, G. L. Hura, J. Teixeira, A. K. Soper and T. Head-Gordon, *Proc. Natl. Acad. Sci. U. S. A.*, 2010, **107**, 14003–14007.
- 10 D. T. Limmer and D. Chandler, *J. Chem. Phys.*, 2011, **135**, 134503.
- 11 V. Molinero and E. B. Moore, *J. Phys. Chem. B*, 2009, **113**, 4008.
- 12 E. B. Moore and V. Molinero, *Nature*, 2011, **479**, 506.
- 13 F. Sciortino, I. Saika-Voivod and P. H. Poole, *Phys. Chem. Chem. Phys.*, 2011, **13**, 19759.
- 14 Y. Liu, A. Z. Panagiotopoulos and P. G. Debenedetti, *J. Chem. Phys.*, 2009, **131**, 104508; Y. Liu, J. C. Palmer, A. Z. Panagiotopoulos and P. G. Debenedetti, *J. Chem. Phys.*, 2012, **137**, 214505.
- 15 D. Banerjee, S. N. Bhat, S. V. Bhat and D. Leporini, *Proc. Natl. Acad. Sci. U. S. A.*, 2009, **106**, 11448–11452.
- 16 S. H. Chen, L. Liu, E. Fratini, P. Baglioni, A. Faraone and E. Mamontov, *Proc. Natl. Acad. Sci. U. S. A.*, 2006, **103**, 9012–9016.
- 17 D. A. Turton, J. Hunger, G. Hefter, R. Buchner and K. Wynne, *J. Chem. Phys.*, 2008, **128**, 161102–5.
- 18 D. A. Turton, C. Corsaro, M. Candelaresi, A. Brownlie, K. R. Seddon, F. Mallamace and K. Wynne, *Faraday Discuss.*, 2011, **150**, 493–504.
- 19 L. Liu, S. H. Chen, A. Faraone, C. W. Yen and C. Y. Mou, *Phys. Rev. Lett.*, 2005, **95**, 117802.
- 20 S. H. Chen, F. Mallamace, C. Y. Mou, M. Broccio, C. Corsaro, A. Faraone and L. Liu, *Proc. Natl. Acad. Sci. U. S. A.*, 2006, **103**, 12974–12978.
- 21 F. Mallamace, M. Broccio, C. Corsaro, A. Faraone, D. Majolino, V. Venuti, L. Liu, C. Y. Mou and S. H. Chen, *Proc. Natl. Acad. Sci. U. S. A.*, 2007, **104**, 424–428.
- 22 F. Mallamace, *Proc. Natl. Acad. Sci. U. S. A.*, 2009, **106**, 15097–15098.
- 23 P. Kumar, S. V. Buldyrev, S. R. Becker, P. H. Pool, F. W. Starr and H. E. Stanley, *Proc. Natl. Acad. Sci. U. S. A.*, 2007, **104**, 9575–9579.
- 24 L. Xu, F. Mallamace, Z. Y. Yan, F. W. Starr, S. V. Buldyrev and H. E. Stanley, *Nat. Phys.*, 2009, **5**, 565–569.
- 25 F. Mallamace, C. Branca, C. Corsaro, N. Leone, J. Spooren, H. E. Stanley and S. H. Chen, *J. Phys. Chem. B*, 2010, **114**, 1870–1878.
- 26 P. W. Bridgman, *Proc. Am. Acad. Arts Sci.*, 1912, **47**, 441–558.
- 27 T. Grindley and J. E. Lind, *J. Chem. Phys.*, 1971, **54**, 3983–3989.
- 28 G. S. Kell, *J. Chem. Eng. Data*, 1975, **20**, 97–105.
- 29 G. S. Kell and E. Whalley, *J. Chem. Phys.*, 1975, **62**, 3496–3503.
- 30 C. M. Sorensen, *J. Chem. Phys.*, 1983, **79**, 1455–1461.
- 31 D. E. Hare and C. M. Sorensen, *J. Chem. Phys.*, 1986, **84**, 5085–5089.
- 32 D. E. Hare and C. M. Sorensen, *J. Chem. Phys.*, 1987, **87**, 4840–4845.
- 33 O. Mishima, *J. Chem. Phys.*, 2010, **133**, 144503.
- 34 F. Mallamace, C. Branca, M. Broccio, C. Corsaro, C. Y. Mou and S. H. Chen, *Proc. Natl. Acad. Sci. U. S. A.*, 2007, **104**, 18387–18391.
- 35 R. J. Speedy and C. A. Angell, *J. Chem. Phys.*, 1976, **65**, 851–858.
- 36 H. Kanno and C. A. Angell, *J. Chem. Phys.*, 1979, **70**, 4008–4016.
- 37 W. D. Wilson, *J. Acoust. Soc. Am.*, 1959, **31**, 1067–1072.
- 38 C. W. Lin and J. P. M. Trusler, *J. Chem. Phys.*, 2012, **136**, 094511.
- 39 E. Tombari, C. Ferrari and G. Salvetti, *Chem. Phys. Lett.*, 1999, **300**, 749–751.
- 40 K. R. Harris and P. J. Newitt, *J. Chem. Eng. Data*, 1997, **42**, 346–348.
- 41 NIST Chemistry WebBook. <http://webbook.nist.gov/chemistry/fluid/2008>.
- 42 F. Mallamace, C. Corsaro and H. E. Stanley, *Sci. Rep.*, 2012, **2**, 993.
- 43 K. Binder and W. Kob, *Glassy Materials and Disordered Solids*, World Scientific, River Edge, NJ, 2005.
- 44 J. Jonas, *Science*, 1982, **216**, 1179–1184.
- 45 H. Tyrrell and K. Harris, *Diffusion in liquids: A Theoretical and Experimental Study*, Butterworth Publishers, London, Boston, 1980.
- 46 S. Sastry, P. G. Debenedetti and S. H. Stillinger, *Nature*, 1998, **393**, 554–557.
- 47 V. Lubchenko and P. Wolynes, *Annu. Rev. Phys. Chem.*, 2007, **58**, 235–266.
- 48 G. Adam and J. Gibbs, *J. Chem. Phys.*, 1965, **43**, 139–146.
- 49 F. H. Stillinger, *Science*, 1995, **267**, 1935–1939.
- 50 F. Mallamace, C. Branca, C. Corsaro, N. Leone, J. Spooren, S. H. Chen and H. E. Stanley, *Proc. Natl. Acad. Sci. U. S. A.*, 2010, **107**, 22457–22462.
- 51 A. Scala, F. W. Starr, E. La Nave, F. Sciortino and H. E. Stanley, *Nature*, 2000, **406**, 166–169.
- 52 C. A. Angell, E. D. Finch, L. A. Woolf and P. Bach, *J. Chem. Phys.*, 1976, **65**, 3063–3066.

Faraday Discussions

- 53 M. Matubayasi, C. Wakai and M. Nakahara, *Phys. Rev. Lett.*, 1997, **78**, 2573–2576.
- 54 E. M. Purcell, H. C. Torrey and R. V. Pound, *Phys. Rev.*, 1946, **69**, 37.
- 55 F. Bloch, *Phys. Rev.*, 1946, **70**, 460.
- 56 E. D. Becker, in *Encyclopedia of Nuclear Magnetic Resonance*, ed. D. M. Grant and R. K. Harris, Wiley, Chichester, 1996, p. 2409.
- 57 F. Mallamace, C. Corsaro, M. Broccio, C. Branca, N. González-Segredo, J. Spooren, S.-H. Chen and H. E. Stanley, *Proc. Natl. Acad. Sci. U. S. A.*, 2008, **105**, 12725–12729.
- 58 J. C. Hindman, *J. Chem. Phys.*, 1966, **44**, 4582–4592.
- 59 C. A. Angell, J. Shuppert and J. C. Tucker, *J. Phys. Chem.*, 1973, **77**, 3092–3099.